JAMA Neurology | Original Investigation

Congenital Zika Virus Infection
Beyond Neonatal Microcephaly

Adriana Suely de Oliveira Melo, MD, PhD; Renato Santana Aguiar, PhD; Melania Maria Ramos Amorim, MD, PhD; Monica B. Arruda, PhD; Fabiana de Oliveira Melo, MD; Suelem Taís Clementino Ribeiro, MD; Alba Gean Medeiros Batista, MD; Thales Ferreira, MD; Mayra Pereira dos Santos, MD; Virgínia Vilar Sampaio, MD; Sarah Rogéria Martins Moura, MD; Luciana Portela Rabello, MD; Clarissa Emanuelle Gonzaga, MD; Gustavo Malinger, MD; Renato Ximenes, MD; Patricia Soares de Oliveira-Szejnfeld, MD; Fernanda Tovar-Moll, MD, PhD; Leila Chimelli, MD, PhD; Paola Paz Silveira, MSc; Rodrigo Delvechio, MSc; Luiza Higa, PhD; Loraine Campanati, PhD; Rita M. R. Nogueira, PhD; Ana Maria Bispo Filippis, PhD; Jacob Szejnfeld, MD, PhD; Carolina Moreira Voloch, PhD; Orlando C. Ferreira Jr, MD, PhD; Rodrigo M. Brindeiro, PhD; Amilcar Tanuri, MD, PhD

IMPORTANCE Recent studies have reported an increase in the number of fetuses and neonates with microcephaly whose mothers were infected with the Zika virus (ZIKV) during pregnancy. To our knowledge, most reports to date have focused on select aspects of the maternal or fetal infection and fetal effects.

OBJECTIVE To describe the prenatal evolution and perinatal outcomes of 11 neonates who had developmental abnormalities and neurological damage associated with ZIKV infection in Brazil.

DESIGN, SETTING, AND PARTICIPANTS We observed 11 infants with congenital ZIKV infection from gestation to 6 months in the state of Paraíba, Brazil. Ten of 11 women included in this study presented with symptoms of ZIKV infection during the first half of pregnancy, and all 11 had laboratory evidence of the infection in several tissues by serology or polymerase chain reaction. Brain damage was confirmed through intrauterine ultrasonography and was complemented by magnetic resonance imaging. Histopathological analysis was performed on the placenta and brain tissue from infants who died. The ZIKV genome was investigated in several tissues and sequenced for further phylogenetic analysis.

MAIN OUTCOMES AND MEASURES Description of the major lesions caused by ZIKV congenital infection.

RESULTS Of the 11 infants, 7 (63.6%) were female, and the median (SD) maternal age at delivery was 25 (6) years. Three of 11 neonates died, giving a perinatal mortality rate of 27.3%. The median (SD) cephalic perimeter at birth was 31 (3) cm, a value lower than the limit to consider a microcephaly case. In all patients, neurological impairments were identified, including microcephaly, a reduction in cerebral volume, ventriculomegaly, cerebellar hypoplasia, lissencephaly with hydrocephalus, and fetal akinesia deformation sequence (ie, arthrogryposis). Results of limited testing for other causes of microcephaly, such as genetic disorders and viral and bacterial infections, were negative, and the ZIKV genome was found in both maternal and neonatal tissues (eg, amniotic fluid, cord blood, placenta, and brain). Phylogenetic analyses showed an intrahost virus variation with some polymorphisms in envelope genes associated with different tissues.

CONCLUSIONS AND RELEVANCE Combined findings from clinical, laboratory, imaging, and pathological examinations provided a more complete picture of the severe damage and developmental abnormalities caused by ZIKV infection than has been previously reported. The term *congenital Zika syndrome* is preferable to refer to these cases, as microcephaly is just one of the clinical signs of this congenital malformation disorder.

JAMA Neurol. 2016;73(12):1407-1416. doi:10.1001/jamaneurol.2016.3720
Published online October 3, 2016. Corrected on October 24, 2016.

Editorial page 1395

Supplemental content

CME Quiz at jamanetworkcme.com and CME Questions 1508

Author Affiliations: Author affiliations are listed at the end of this article.

Corresponding Author: Amilcar Tanuri, MD, PhD, Laboratório de Virologia Molecular, Departamento de Genética, Instituto de Biologia, Universidade Federal do Rio de Janeiro, CCS Bloco A Sala 121, Rio de Janeiro 21941-902, Brazil (atanuri1@gmail.com).

The birth prevalence of neonatal microcephaly and other central nervous system malformations greatly increased between 2015 and mid-2016 in Brazil.[1-3] Several reports[1,2,4-6] suggested an association between these findings and Zika virus (ZIKV) infection during outbreaks in Brazil and French Polynesia. Zika virus arrived in Brazil through the northeastern region and spread primarily to the states of Bahia, Pernambuco, and Paraíba.[7,8] It is a flavivirus transmitted by *Aedes* mosquitoes, and the infection in humans usually presents with 1 or more of the following symptoms: low-grade fever, arthralgia, rash, headache, and myalgia.[9,10] However, most infections are asymptomatic.[2] Neurological disorders associated with ZIKV infection include congenital microcephaly and adult manifestations such as Guillain-Barré syndrome, acute myelitis, and meningoencephalitis.[1,11-13]

To our knowledge, most of the previously reported neonatal microcephaly cases (eg, birth head circumference less than the third percentile for sex and gestational age[14]) were associated with the manifestation of ZIKV infection symptoms in the first trimester of pregnancy.[1,2,5] Microcephaly was not the only fetal abnormality observed, and other findings were documented later. Fetal neurosonography and magnetic resonance imaging (MRI) have also showed diffuse calcification in the subcortical parenchyma and thalamic areas, ventriculomegaly, lissencephaly, and pachygyria (ie, smooth brains with reduced gyral ridges).[6] Nevertheless, to our knowledge, a systematic follow-up of clinical and morphological features of these cases along with anatomic and pathological descriptions associated with congenital ZIKV infection has not been reported. In addition, the mechanism by which the ZIKV infection can cause fetal brain damage is not known, and some reports suggest that the virus is able to evade the normal immunoprotective responses of the placenta.[15] Zika virus is not the only pathogen associated with neonate microcephaly. Other viruses, such as cytomegalovirus, herpes simplex virus types 1 and 2, varicella-zoster virus, human immunodeficiency virus, and chikungunya virus, have also been described to cause congenital malformations.[16,17]

We report the follow-up of 11 infants with congenital ZIKV infections in Brazil. Zika virus was identified in the amniotic fluid (AF), placenta, cord blood, and neonatal tissues collected postmortem for all patients. We combined information from clinical evaluations and diagnostic laboratory and imaging findings with postmortem anatomical and pathological data to more completely describe the lesions caused by ZIKV congenital infection and document its effect in different target tissues and organs during intrauterine development.

Key Points

Question Which kind of abnormalities are present in babies from pregnant women exposed to the Zika virus?

Findings In this follow-up of 11 infants with congenital Zika virus infection, we identified neurological impairments, including microcephaly, a reduction in cerebral volume, ventriculomegaly, cerebellar hypoplasia, lissencephaly with hydrocephalus, and fetal akinesia deformation sequence (ie, arthrogryposis).

Meaning These data reinforce that microcephaly is one of several neurological impairments observed in infants exposed to the Zika virus, and complementary examinations, such as ultrasonography and magnetic resonance imaging, should be performed to better characterize the clinical manifestations of Zika virus infection.

Methods

Case Selection

Between October 2015 and February 2016, several cases of suspected fetal microcephaly associated with maternal ZIKV infection in the first half of pregnancy were referred to the fetal medicine service of the Instituto Paraibano de Pesquisa Professor Joaquim Amorim Neto (IPESQ) in Campina Grande, Paraíba, Brazil. This prospective study was conducted in Campina Grande, the second largest city in the state of Paraíba, which has reported the second highest prevalence of microcephaly at birth in Brazil. More than 150 pregnant women with symptoms of ZIKV infection were observed. Eleven of these women were selected to study because of findings of brain lesions during fetal ultrasound imaging (USG). Amniocentesis was performed in all women for laboratory confirmation of ZIKV infection by polymerase chain reaction (PCR). These women were observed until they gave birth, and additional imaging and other samples after birth (eg, AF, cord blood, and placenta samples) were collected to confirm the presence of the virus in the newborns. Three of 11 babies died after birth, and the remaining neonates are still alive. Two mothers gave consent for autopsies, and several tissues were collected for PCR testing as well histopathology studies (**Table**). This study was approved by Hospital Pedro I Institutional Review Board. Written informed consent was obtained from all mothers.

Imaging

After initial evaluation, 3 fetal medicine specialists continued to monitor fetal anatomy, biometrical indices, AF levels, placental health, and umbilical and middle cerebral artery blood flow. Abdominal and transvaginal ultrasonographic examination was performed for all women per Brazilian public health recommendations, and amniocentesis was performed in all mothers to investigate the cause of neurological damage. Ultrasonography-guided transabdominal amniocentesis was performed, and about 5 mL of AF was aspirated and stored at −80°C. Doppler studies were conducted to investigate umbilical artery and/or middle cerebral artery abnormalities for all women. Examinations were performed on Accuvix XG and WS80 (Samsung) with 2- to 9-mHz probes. Three-dimensional construction was also available in some cases.

Magnetic resonance imaging of the fetus was performed on a MAGNETOM Skyra 3-T scanner (Siemens Healthcare) or on a MAGNETOM Espree 1.5-T scanner (Siemens Healthcare) with an 8-channel body coil and standard acquisition protocols. Brain 16-channel multislice computed tomography scanning (Siemens Healthcare) and/or brain MRI (Espree 1.5 T) were performed on neonates. A postmortem brain computed tomography scan and MRI were conducted using a 64-channel

Table. Characteristics of Mothers and Fetuses or Neonates With Microcephaly

Patient No., Sex	Maternal Age, y	Acute ZIKV Symptoms (GT of First Appearance, wk)	GT of First Image With Lesion, wk	PCR Diagnosis of Amniocentesis (GT, wk)	GT Delivery, wk (CP, cm)	Newborn Outcome	PCR Diagnosis at Birth (AF, CB, and PL)	Postmortem Tissue PCR (PL, BR, CB, SC, and LG)	ZIKV Rapid Test Result for CB	
									IgG	IgM
1, M	23	Rash, itching, and arthralgia (18)	20	Pos (20)	41 (36.5)	Deceased	Neg	Pos (BR)	Pos	Neg
2, F	34	Rash, arthralgia, and conjunctivitis (8)	20	Pos (20)	41 (30.5)	Alive	Neg	NA	Pos	Neg
3, M	29	Rash, arthralgia, and itching (12)	24	Pos (24)	41 (31.5)	Alive	Pos (AF)	NA	NA	NA
4, F	25	NA	23	Pos (23)	39 (35.5)	Alive	NA	Pos (AF)	NA	NA
5, F	18	Rash (10)	37	Pos (37)	40 (29)	Alive	Neg	NA	NA	NA
6, F	19	Rash, headache, and asthenia (6)	20	Pos (20)	39 (33.0)	Alive	NA	Pos (AF)	NA	NA
7, F	31	Rash, itching, and feet edema (7)	17	Neg (17)	36 (35.0)	Deceased	Pos (AF)	Pos (BR, CR, SC, LG)	NA	NA
8, M	19	Rash, asthenia, and itch (10)	35	Neg (35)	41 (32.5)	Alive	Pos (PL)	Neg	NA	NA
9, M	15	Rash, itch, and arthralgia (8)	25	Neg (25)	34 (27.0)	Deceased	Pos (PL, CB)	Neg (BR,CR)	NA	NA
10, F	29	Rash and itching (11)	20	Neg (20)	40 (29.0)	Alive	Neg	NA	Pos	Neg
11, F	26	Rash and headache (9)	22	Neg (22)	38 (29.0)	Alive	Neg	NA	Pos	Neg
Female, 7 of 11 (63.6%)	Median (SD) age, 25 (6) y	Median (SD) GT, 9.5 (3.4) wk	Median (SD) GT, 22 (6.4) wk	Pos on AF PCR, 6 of 11 (54.5%); median (SD) GT, 22 (6.4) wk	Median (SD) GT, 39 (2.3) wk; median (SD) CP, 31 (3) cm	Mortality, 3 of 11 (27.3%)	NA	NA	NA	NA

Abbreviations: AF, amniotic fluid; BR, brain; CB, cord blood; CP, cephalic perimeter; GT, gestational time; LG, lung; NA, not applicable; Neg, negative; PCR, polymerase chain reaction; PL, placenta; Pos, positive; SC, spinal cord; ZIKV, Zika virus.

multislice computed tomography scanner (General Electrics) and an Achieva 3-T TX scanner (Philips), respectively.

Autopsy and Sample Collection

Amniotic fluid was collected in 8 of 11 neonates by amniocentesis. Placenta, AF, and cord blood samples were collected at delivery. Postmortem tissues from the brain, cerebellum, cord blood, spinal cord, and lung were also collected from deceased babies. Full autopsies were performed less than 8 hours after death. Samples were either fixed in 10% buffered formalin and embedded in paraffin for histopathology analysis or stored in RNAlater (Thermo Fisher Scientific) for further investigations of pathogens. Representative areas of formalin fixed tissues were processed for paraffin embedding. Histological sections were stained with hematoxylin-eosin. From selected areas, immunohistochemical reactions were performed using the following antibodies and dilutions: anti-glial fibrillary acidic protein (1:500), anti-neurofilament (1:2000), anti-CD3 (1:1000), anti-CD20 (1:1000), and anti-CD68 (1:1000).

ZIKV Infection Diagnosis

Viral RNA was extracted from AF and blood using the QIAamp viral RNA mini kit (Qiagen) according to the manufacturer's recommendations. Fifty milligrams of organ tissues, such as brain, lung, and placenta, were disrupted using TissueRuptor (Qiagen) using 325 µL of RTL buffer from the RNEasy plus mini kit (Qiagen), according to the manufacturer's protocol. RNA was extracted from 10 mg of tissue from the placenta, lungs, heart, skin, spleen, thymus, liver, kidneys, and cerebral cortex with the use of a TRIzol Plus RNA purification kit (Thermo Fisher Scientific). Real-time reverse-transcription PCRs (RT-PCRs) were performed for the detection of ZIKV RNA (*NS5* gene) and 1-step RT-PCR for the detection of the envelope-protein coding region (350 base pairs) as described previously.[18] The envelope gene of positive samples for ZIKV RT-PCR was sequenced for further phylogenetic analysis. Viral complementary DNA was amplified using the SuperScript III One-Step RT-PCR system with platinum *Taq* DNA polymerase (Thermo Fisher Scientific) following the manufacturer's protocol. A fragment of 350 base pairs containing the *env* gene was amplified using primers 5′-TTGGTCATGATACTGCTGATTGC-3′ (forward) and 5′-CCACTAACGTTCTTTTGCAGACAT-3′ (reverse) and subjected to nucleic acid sequence analysis with the same primers by using the ABI 3130 Genetic Analyzer (Applied Biosystems). Raw sequence data were aligned and edited by the SeqMan module of LaserGene (DNASTAR). Amino acid sequence alignment was performed using the Clustal W package. Serological tests against ZIKV were performed using the rapid-test dual path platform Zika IgM/IgG from Chembio (Medford). We previously validated this rapid test with sera from ZIKV-positive babies (patients 1 and 2 in the Table) and a sero-

conversion sera panel from adults infected with ZIKV in the state of Rio de Janeiro, Brazil (eFigure 1 in the Supplement). Moreover, this rapid test has been previously validated with a bona fide ZIKV seroconversion panel from adults infected with ZIKV in the state of Rio de Janeiro. Findings from patients 1 and 2 also validated the use of cord blood as a diagnostic matrix for the Chembio dual path platform. Furthermore, the manufacturer reports the specificity for DENV, YFV, and WNV proteases were all greater than 90%. Phylogenetic analysis methods are described in eAppendix 1 in the Supplement.

Results

Cases Series Characteristics

Eleven pregnant women with confirmed ZIKV diagnoses showing some fetal abnormality in brain development by abdominal ultrasonographic examination were enrolled in this study after providing informed consent (Table). Then, during the intrauterine period, RT-PCR of the AF confirmed the ZIKV diagnosis in 6 of 11 women (patients 1-6 in Table). The remaining infants were diagnosed after birth through RT-PCR using AF, placenta tissues, or cord blood collected after delivery, with the exception of patients 10 and 11, from whom only a small volume of cord blood was available. However, both patients were included in the study on the basis of a strong IgG anti-ZIKV response obtained by the Chembio dual path platform ZIKV IgG/IgM rapid test. Patients 10 and 11 are considered suspect cases because of suggestive imaging findings, a maternal history of ZIKV infection symptoms during pregnancy, and strong IgG anti-ZIKV immune titles (eFigure 1 in the Supplement).

The ZIKV genome was identified in postmortem tissues in patient 1 (brain) and patient 7 (brain, cerebellum, spinal cord, and lung). Of note, patient 1 had more severe brain damage and a higher viral load in brain tissues compared with patient 7. Additional laboratory tests conducted in their mothers excluded diabetes and other chronic diseases, such as blood pressure–related disorders. Other causes of microcephaly, such as drug use, alcohol consumption, smoking, or medication, were also excluded. Test results for other arboviruses, such as dengue virus and chikungunya, were found to be negative by enzyme-linked immunosorbent assay and PCR examination in blood and AF. Tests for syphilis, toxoplasmosis, human immunodeficiency virus, measles, rubella, cytomegalovirus, and herpes simplex panels were also negative for all infants, as were specific human immunodeficiency virus, syphilis, cytomegalovirus, and parvovirus B19 screens.

Fetal USG was performed 3 to 6 times on each pregnant woman, depending on the severity of findings. Magnetic resonance imaging was also performed if fetal cerebral malformations were detected. At the time of this submission, all 11 patients were delivered. Three infants died after delivery (within 48 hours of life), and 2 mothers allowed full autopsy. The summary of demographic information and clinical and laboratory findings are presented in the Table. The median (SD) maternal age was 25 (6) years. Five of 11 mothers (45.5%) were primigravidas, while the median number of births for the remaining mothers was 2. All pregnant women except the mother of patient 1 had a history of skin rash at the beginning of pregnancy, appearing at a median (SD) gestational time of 9.5 (3.4) weeks, suggesting an early ZIKV infection. The median (SD) gestational age at delivery was 39 (2.6) weeks, and labor was induced for most women. All infants were aged 2 to 6 months at the time of submission. Three of 11 neonates died, giving a perinatal mortality rate of 27.3%. The median (SD) cephalic perimeter at birth was 31 (3) cm, a value lower than the limit to consider a microcephaly case. However, we found newborns with severe brain lesions with normal cephalic perimeter.

Imaging Findings

The most common finding on abdominal and transvaginal USG was severe cerebral atrophy associated with fetal microcephaly, which was found in 9 patients. Ventriculomegaly was another frequent finding, appearing in 10 patients, and was mild, moderate, or severe and usually asymmetric. The head circumference was less than 2 SDs for gestational age in most infants; however, normal or enlarged head circumference with severe ventriculomegaly was found in 2 patients (median [SD; range] of 31 [3; 27-36.5] cm). Hypoplasia of the cerebellar vermis and cerebellum occurred in 9 patients. We found unilateral microphthalmia and bilateral cataracts in patient 1 but could not visualize the corpus callosum and the thalami. Fetal akinesia deformation sequence (FADS) or arthrogryposis was found in 3 infants, and all 3 died after delivery (patients 1, 7, and 9). Polyhydramnios was found in patient 7, who also developed severe maternal respiratory distress necessitating therapeutic interruption of pregnancy at 36 weeks. Oligohydramnios was observed in patient 2. Doppler flow velocimetry indices (umbilical and middle cerebral artery) were normal in all patients. Other USG findings included calcifications in several regions in the brain, cerebellum, and brainstem in addition to fetal restriction growth. We also identified frontal bone plane, hypertelorism, and enlargement of the posterior fossa, interhemispheric space, and subarachnoid space. The earliest sonographic findings were FADS for patient 7 and head circumferences less than the third percentile for patients 2 and 7 at 17 weeks.

Complementing the USG findings, fetal and/or postnatal MRI and CT findings showed additional abnormalities, including callosal hypoplasia, reduced cerebral volume, abnormal cortical development, and subcortical calcifications, which were found in all patients. Although abnormal cortical development could be identified in every patient, changes included less severe gyral disorganization (patients 3 and 6-8), pachygyria (patients 2, 5, and 9-11), and lissencephaly (patients 1 and 4). Morphological abnormalities of basal ganglia and thalamus and hypodevelopment of the brainstem and cerebellum were observed in most patients. **Figure 1** summarizes the typical developmental abnormalities identified in different patients. Imaging findings in each patient are summarized in eTables 1 and 2 in the Supplement. **Figure 2** shows fetal and postmortem imaging findings of patients 1 and 7.

Pathology Findings

Tissues collected post mortem (patients 1 and 7) were processed for further histopathological investigations. On mac-

Figure 1. Typical Imaging Findings

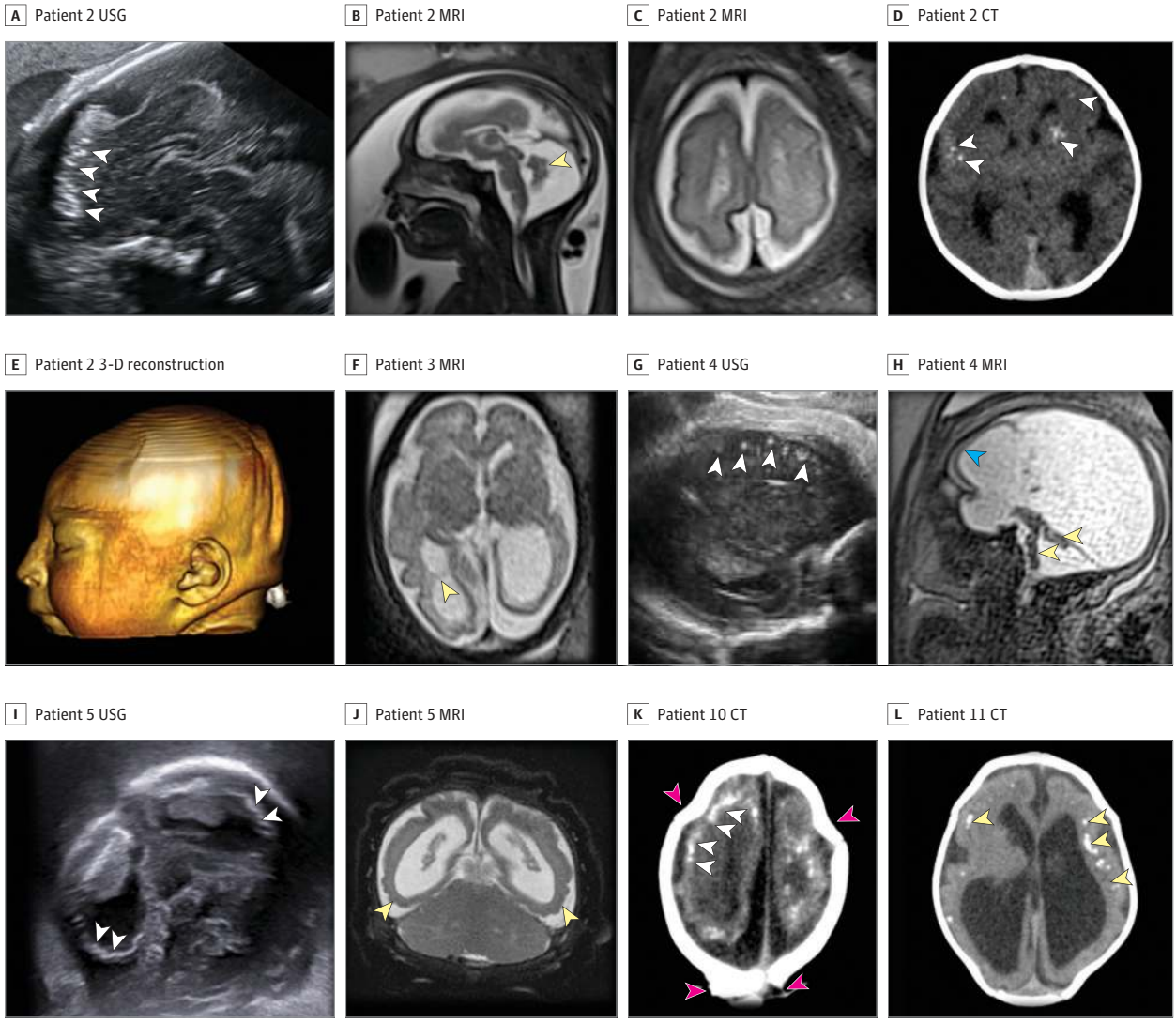

Patients 2 (A-E), 3 (F), 4 (G, H), 5 (I, J), 10 (K), and 11 (L) underwent fetal ultrasound imaging (USG), magnetic resonance imaging (MRI), and computed tomography (CT). A, Multiple and aligned subcortical calcifications (arrowheads) at 29 weeks' gestation. B, Reduced cerebral volume, callosal hypoplasia, vermian hypoplasia (arrowhead), and enlarged cisterna magna. C, Abnormal cortical development (pachygyria). D, Basal ganglia and subcortical calcifications (arrowheads) on postnatal imaging. E, Microcephaly on postnatal 3-dimensional (3-D) reconstruction. F, Abnormal cortical development, ex-vacuo ventriculomegaly, and ventricular septa between the atrium and occipital horn (arrowhead) with hyposignal spots suggestive of calcification in thalamus at 29 weeks' gestation. G, Subcortical calcifications (arrowheads) at 24 weeks' gestation. H, Severe reduction of cerebral parenchyma volume associated with lissencephaly (blue arrowhead) and accentuated hypodevelopment of diencephalon, brainstem, and cerebellum (yellow arrowheads) at 36 weeks' gestation. I, Remarkable hypodevelopment of the cerebral parenchyma and aligned subcortical calcifications (arrowheads) at 37 weeks' gestation. J, Ventriculomegaly and abnormal cortical development with polymicrogyria (arrowheads) on postnatal imaging. K, Subcortical calcifications (white arrowheads) and skull deformity (red arrowheads) on postnatal imaging. L, Reduced cerebral volume, ventriculomegaly, and aligned subcortical calcifications (arrowheads) on postnatal imaging.

roscopic inspection, brain tissue available from patient 1 was a segment of cerebral hemisphere, weighing 38.5 g, including a small segment of the brainstem. It was partly agyric, with congested leptomeninges and occasional shallow sulci (**Figure 3**A). The lateral ventricles were enlarged, with very thin cortex and white matter (eFigure 3 in the Supplement). Neither the basal ganglia nor thalami were identified. Histopathological analyses showed cortical polymicrogyria, small clusters of calcification closer to the ventricular surface (Figure 3B), absence of ependymal lining, and multiple small foci of calcification and degenerate nerve cells in the brainstem (Figure 3C; eFigure 4 in the Supplement). There were occasional meningeal and perivascular lymphocytes in the brainstem. Leptomeningeal glioneuronal heterotopia was observed in the surface of the hemispheres and the brainstem (eFigure 5 in the Supplement).

For patient 7, available brain tissue consisted of 1 cerebral hemisphere weighing 109 g, 1 cerebellar hemisphere

Figure 2. Imaging Findings for Patients 1 and 7

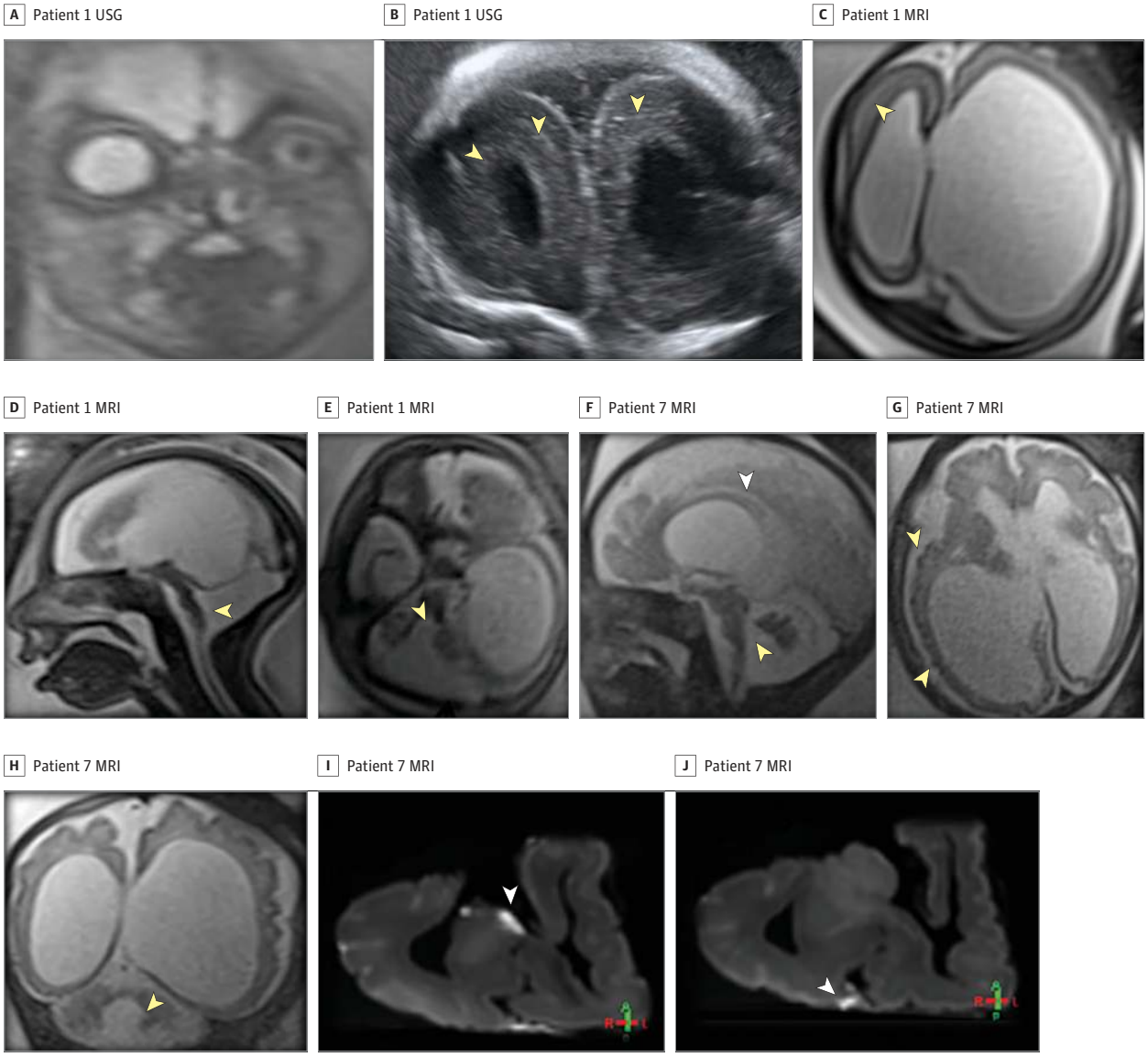

Patients 1 (A-E) and 7 (F-J) underwent fetal ultrasound imaging (USG) and magnetic resonance imaging (MRI). A, Microphthalmia at 29 weeks' gestation. B, Reduced cerebral volume and subcortical calcifications (arrowheads). C, Vetroculomegalia and abnormal cortical development (ie, lissencephaly; arrowhead). D, Brainstem hypoplasia (arrowhead). E, Cerebellum hypoplasia (arrowhead). F, Reduced cerebral volume, vetroculomegalia, callosal hypoplasia (white arrowhead), and brainstem hypoplasia (yellow arrowhead) at 36 weeks' gestation. G, Abnormal cortical development with hyposignal spots suggestive of calcification (arrowheads). H, Cerebellum hypoplasia (arrowhead). I, Abnormal cortical development and brainstem (arrowhead) post mortem. J, Subcortical calcifications (arrowhead) post mortem.

weighing 7 g, the brainstem, and a short segment of the spinal cord. The leptomeninges were thickened and congested with chronic lymphocytic meningitis (Figure 3D). There were shallow sulci, grayish translucent white matter, and enlarged lateral ventricle (Figure 3E; eFigure 2 in the Supplement), showing erosion of the ependyma. The corpus callosum was thin. There were scattered perivascular lymphocytes, histiocytes, gliosis, and a cluster of calcification in the thalamus (Figure 3F). Nerve cell degeneration, coarse and filamentous calcification possibly representing axons, and dendrites were seen in the brainstem (Figure 3G). The cerebellum was hypoplastic (Figure 3H) and had focal cortical dysplasia. Although the sections of the spinal cord could not be well oriented to obtain transverse histological sections, the impression was that there were fewer motor nerve cells than expected. Samples from the paravertebral skeletal muscle showed neurogenic atrophy (data not shown).

The histopathological investigations in both patients 1 and 7 showed predominantly $CD3^+$ lymphocytes (eFigure 6 in the Supplement). Indeed, histiocyte and microglial proliferation, gliosis, and neuronal and axonal degeneration were confirmed with immunohistochemical markers (anti-CD68,

Figure 3. Macroscopic and Histopathologic Findings of Postmortem Brain Tissues of Patients 1 and 7

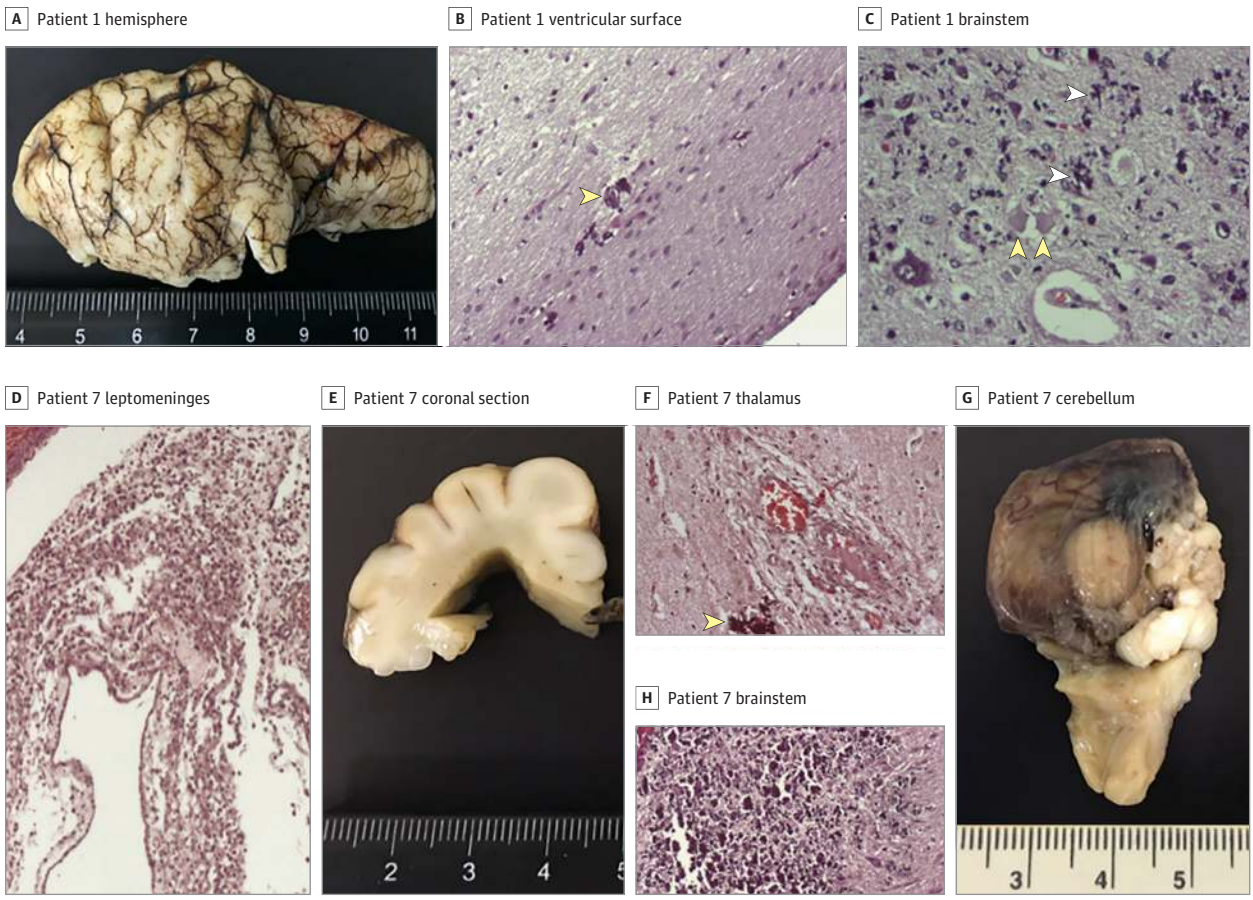

A, Segment of a partly agyric hemisphere, with congested leptomeninges and occasional shallow sulci. B, Small clusters of calcification closer to the ventricular surface (arrowhead) (hematoxylin-eosin, original magnification ×100). C, Multiple small foci of calcification in the brainstem (white arrowheads) and degenerate nerve cells (yellow arrowheads) (hematoxylin-eosin, original magnification ×400). D, Chronic lymphocytic meningitis (hematoxylin-eosin, original magnification ×100). E, Coronal section of the upper part of one hemisphere showing shallow sulci, grayish translucent white matter, and enlarged lateral ventricle (eFigure 2 in the Supplement). F, Thalamus showing scattered perivascular lymphocytes, histiocytes, gliosis, and a cluster of calcification (arrowhead) (hematoxylin-eosin, original magnification ×400). G, Hypoplastic cerebellum and brainstem. H, Coarse calcification in the brainstem (hematoxylin-eosin, original magnification ×400).

anti-glial fibrillary acidic protein antibodies, and anti-neurofilament antibodies, respectively). Two small fragments of the placenta (2.5 × 2.0 cm) from each patient were also examined histologically. Vessel walls in some villi and villous axis were thickened with consequent reduction of their lumens (eAppendix 2 in the Supplement).

Clinical Features

Unilateral ocular abnormalities were observed in patient 10, who presented with a macular chorioretinal scar and perilesional pigmentary mottling. Regarding the neurological development of newborns, our main ocular findings to date have been paresis of the oculomotor and abduces muscles with convergent strabismus and loss of photomotor and consensual reflexes. Others findings included myoclonic seizures, hyporeflexia, cervical hypotonia, paralysis of the diaphragm, and premature closure of the anterior fontanelle.

Phylogenetic Analyses and Intrahost Variation

To evaluate the phylogenetic associations of ZIKV sequences found in these patients and the intrahost variation, we sequenced 350 nucleotide sequences of the envelope gene domain I from patients 1 and 3 to 8 and compared them with other available ZIKV and Spondweni virus sequences from Asia, the Pacific Islands, Africa, and the Americas (eFigure 7 in the Supplement). All African sequences were clustered in 4 monophyletic groups that were separate from the American-Asian-Pacific lineage, supporting the previous findings that Brazilian ZIKV lineages are probably more closely related to Asian-Pacific than to African strains. Our results also support the finding that the American-Asian-Pacific and African lineages could have been isolated for a long time, as the 1966 Malaysian sequence (HQ234449) is the first Asian sequence that derives in the American-Asian-Pacific clade. Several nodes of the tree had low support values, and consequently, the phylogenetic relation of the

clades could not be clearly inferred. The phylogenetic analyses also showed an intrahost variation between ZIKV sequences of different postmortem tissues from patients 1 and 7 that did not group in the same branch (eFigure 7A in the Supplement). Some Brazilian sequences presented a V23I polymorphism at amino acid position 23 of the ZIKV envelope protein (eFigure 7B in the Supplement). Whether this polymorphism results in a different behavior of virus tropism or other virological effects should be investigated further.

Discussion

Our study reports the evaluation of 11 infants exposed to ZIKV infection intrautero and describes their prenatal and postnatal brain lesions and other developmental abnormalities. Patients 1 through 9 had evidence of a positive RT-PCR for ZIKV during gestation and/or after birth. Patients 10 and 11 only had serological evidence of infection, with a suggestion that infection occurred at the time of their gestation. The report demonstrates phenotypic variability in regard to the presence of observed microcephaly as well as the degree of brain damage and affected brain structures with congenital ZIKV infection. Although most infants had microcephaly by head circumference measure, some patients had a measurement that was consistent with their gestational age, as brain atrophy was compensated by an enlargement in ventricular size.[19]

Although there was variable damage resulting from brain lesions associated with ZIKV congenital infection, a common pattern of brain atrophy and changes associated with disturbances in neuronal migration were observed. Some patients presented with mild brain atrophy and calcifications, and others presented with more severe malformations, such as the absence of the thalamus and lissencephaly. Infection caused by ZIKV during pregnancy caused brain damage, mainly characterized by decreased cortical development and atrophy.[6] This cerebral atrophy may be attributable to interference in the formation and neuronal migration during the cerebral embryogenesis that has been described for other congenital infections also associated with malformations of cortical development (particularly toxoplasmosis, rubella, cytomegalovirus, herpes simplex virus complex).[20-22] This is the common pathway that may explain other brain findings and fetal complications caused by ZIKV infection.[23]

Other frequent findings were hypoplasia of the cerebellum and cerebellar vermis, with consequent enlargement of the posterior fossa, calcifications in various brain regions, and hypoplasia of the corpus callosum. The corpus callosum changes may be associated with a decreased number of neuronal cells and/or the interference of the virus in the neuronal migration process, similar to what has been described for human immunodeficiency virus and herpes virus.[24-26] In more severely affected infants, we observed a slender brainstem on fetal MRI, making it impossible for the fetus to breathe normally at birth, with death occurring within hours. Therefore, evaluation of brainstem appearance on fetal MRI may inform the likelihood of survival of the newborn.

In addition to changes in the central nervous system, we also observed FADS, also known as arthrogryposis.[27] In particular, patient 7 presented signs of FADS after 17 weeks of gestation, very early in the fetal development. One hypothesis to explain the early development of FADS could be the interference of ZIKV in the motor neurons migration process, evidenced by histopathological study of patients 1 and 7. Another intrauterine abnormality observed in several patients was polyhydramnios, probably associated with swallowing impairment due to brain injury.[28]

In our study, most of the women demonstrated symptoms of ZIKV infection in the first trimester, which could be associated with the disturbance in neuronal migration processes and the formation of the neural tube. However, in patient 1, one of the most severely affected infants, important brain structures such as the thalamus could not be identified, and the mother reported symptoms of ZIKV infection later than others at 18 weeks of gestation. In fact, this was the only instance in our study in which the mother showed ZIKV symptoms after the first trimester of gestation. Other factors associated with immunity and maternal nutrition could also interfere with ZIKV vertical transmission, as could individual factors that interfere with placental development, and should be further investigated.[15]

Of note, all ZIKV genomes sequenced from fetuses in early pregnancy and newborns belonged to the ZIKV Asian lineage, and they were all related to the viruses identified in the French Polynesian outbreak.[29-31] It was interesting to note that the viral sequences amplified from patients 1 and 7 after birth gained a new substitution, V23I, which is located in the envelope domain I and may be implicated in viral tropism to different tissues. We need to further investigate if this specific variation is associated with neuropathogenesis.

Our study had limitations. One limitation was that most of the imaging was performed during gestation, and further MRI examinations should be performed after delivery to investigate brain damage associated with the neuron-motor development of the child. Another limitation was that most of the ZIKV diagnoses were performed after clinical symptoms during the pregnancy.

Conclusions

The presence of ZIKV in AF during gestation indicates that AF is a valuable fluid for prenatal diagnoses. The finding of ZIKV sequences in placenta and cord blood in some of our newborns provides additional evidence of the vertical transmission of the virus during pregnancy. Unlike the findings reported by others, we did not observe changes in umbilical and cerebral blood flow, even in the most serious cases.[2] However, other questions concerning virus pathogenesis and consequences to fetal development remain unanswered. What seems to be universal is that microcephaly is not the sole finding but is a consequence of several brain injuries. Growth restriction and other damages, such as ophthalmologic alterations, were observed in neonates.[32,33] Indeed, we observed a pronounced ventriculomegaly in most patients that could in-

fluence the observed microcephaly. Perhaps some infants do have damages that impair cerebrospinal fluid flow and then have the obstructive type of ventricular enlargement. Based on that, we recommend using the term *congenital Zika syndrome* instead of *microcephaly associated with Zika virus infection*, which involves a spectrum of changes, including other neurological and fetal development manifestations.

Our observations add ZIKV to a list of other pathogens associated with congenital syndromes during pregnancy. However, based on confirmed ZIKV-associated cases of microcephaly reported by the Brazilian Ministry of Health, the northeastern region of Brazil has a 10 times larger incidence of confirmed cases compared with the rest of Brazil as well other Latin American countries where ZIKV circulates. This fact suggests that there must be some additional unknown factor to enhance ZIKV fetal infection in this region. Coinfections as well as environmental factors should be explored to clear this unexpected finding.

ARTICLE INFORMATION

Accepted for Publication: July 19, 2016.

Correction: This article was corrected on October 24, 2016, to fix the corresponding author's email address.

Published Online: October 3, 2016. doi:10.1001/jamaneurol.2016.3720

Author Affiliations: Instituto de Pesquisa Professor Amorim Neto (IPESQ), Campina Grande, Paraíba, Brazil (A. S. Melo, Amorim, F. d. Melo); Instituto de Saúde Elpidio de Almeida, Campina Grande, Paraíba, Brazil (A. S. Melo, Amorim, F. d. Melo, Ribeiro, dos Santos); Faculdade de Ciências Médicas de Campina Grande, Campina Grande, Paraíba, Brazil (A. S. Melo, Amorim, Ribeiro, Sampaio, Moura, Rabello); Hospital Municipal Pedro I, Campina Grande, Paraíba, Brazil (A. S. Melo, Batista, Sampaio, Moura, Rabello, Gonzaga); Departamento de Genética, Instituto de Biologia, Universidade Federal do Rio de Janeiro, Rio de Janeiro, Rio de Janeiro, Brazil (Aguiar, Arruda, Silveira, Delvechio, Higa, Voloch, O. C. Ferreira, Brindeiro, Tanuri); Universidade Federal de Campina Grande, Paraíba, Brazil (Amorim, T. Ferreira); Division of Ultrasound in Obstetrics and Gynecology, Lis Maternity Hospital, Tel Aviv Sourasky Medical Center, Sackler Faculty of Medicine, Tel Aviv University, Tel Aviv, Israel (Malinger); Fundação de Medicina Fetal Latino Americana, Campinas, São Paulo, Brazil. (Ximenes); Fundação Instituto de Pesquisa e Ensino de Diagnostico por Imagem, Universidade Federal de São Paulo, São Paulo, Brazil (de Oliveira-Szejnfeld); Instituto de Ciências Biomédicas, Universidade Federal do Rio de Janeiro, Rio de Janeiro, Brazil (Tovar-Moll, Campanati); Instituto D'Or de Pesquisa e Ensino, Rio de Janeiro, Rio de Janeiro, Brazil (Tovar-Moll); Laboratório de Neuropatologia do Instituto Estadual do Cérebro Paulo Niemeyer, Rio de Janeiro, Brazil (Chimelli); Laboratório de Flavivírus, Instituto Oswaldo Cruz, Fundação Oswaldo Cruz, Rio de Janeiro, Rio de Janeiro, Brazil (Nogueira, Filippis); Departamento de Diagnóstico por Imagem, Universidade Federal de São Paulo, São Paulo, Brazil (Szejnfeld).

Author Contributions: Drs Tanuri and Melo had full access to all the data in the study and take responsibility for the integrity of the data and the accuracy of the data analysis. Drs A. S. Melo and Aguiar contributed equally.
Concept and design: Tanuri, Melo, Aguiar.
Acquisition, analysis, or interpretation of data: A. S. Melo, Aguiar, Amorim, Arruda, F. d. Melo, Ribeiro, Batista, Ferreira, dos Santos, Sampaio, Moura, Rabello, Gonzaga, Malinger, Ximenes, de Oliveira-Szejnfeld, Tovar-Moll, Chimelli, Silveira, Delvechio, Higa, Campanati, Nogueira, Filippis, Szejnfeld, Voloch, Ferreira, Brindeiro.
Drafting of the manuscript: Tanuri, Melo, Aguiar, Amorim, de Oliveira-Szejnfeld, Tovar-Moll, Chimelli, Campanati, Voloch, Brindeiro.
Critical revision of the manuscript for important intellectual content: A. S. Melo, Aguiar, Amorim, Arruda, F. d. Melo, Ribeiro, Batista, Ferreira, dos Santos, Sampaio, Moura, Rabello, Gonzaga, Malinger, Ximenes, de Oliveira-Szejnfeld, Tovar-Moll, Silveira, Delvechio, Higa, Campanati, Nogueira, Filippis, Szejnfeld, Ferreira.
Statistical analysis: Tovar-Moll, Voloch.
Obtaining funding: Tanuri, Melo, Aguiar, Campanati.
Administrative, technical, or material support: A. S. Melo, Aguiar, Amorim, Arruda, F. d. Melo, Ribeiro, Ferreira, Sampaio, Moura, Rabello, Malinger, Ximenes, de Oliveira-Szejnfeld, Tovar-Moll, Silveira, Higa, Campanati, Nogueira, Filippis, Szejnfeld, Voloch, Ferreira, Brindeiro.
Study supervision: Tanuri, A. S. Melo.

Conflict of Interest Disclosures: None reported.

Funding/Support: This study was supported by Consellho Nacional de Desenvolvimento e Pesquisa, Fundação de Amparo a Pesquisa do Estado do Rio de Janeiro, Coordenação de Aperfeiçoamento de Pessoal de Nível Superior, and Prefeitura Municipal de Campina Grande.

Role of the Funder/Sponsor: The funders had no role in the design and conduct of the study; collection, management, analysis, and interpretation of the data; preparation, review, or approval of the manuscript; and decision to submit the manuscript for publication.

REFERENCES

1. Calvet G, Aguiar RS, Melo AS, et al. Detection and sequencing of Zika virus from amniotic fluid of fetuses with microcephaly in Brazil: a case study. *Lancet Infect Dis*. 2016;16(6):653-660.

2. Brasil P, Pereira JP Jr, Raja Gabaglia C, et al. Zika virus infection in pregnant women in Rio de Janeiro: preliminary report [published online March 4, 2016]. *N Engl J Med*.

3. Malone RW, Homan J, Callahan MV, et al; Zika Response Working Group. Zika virus: medical countermeasure development challenges. *PLoS Negl Trop Dis*. 2016;10(3):e0004530.

4. Cauchemez S, Besnard M, Bompard P, et al. Association between Zika virus and microcephaly in French Polynesia, 2013-15: a retrospective study. *Lancet*. 2016;387(10033):2125-2132.

5. Faria NR, Azevedo RdoS, Kraemer MUG, et al. Zika virus in the Americas: early epidemiological and genetic findings. *Science*. 2016;352(6283):345-349.

6. Mlakar J, Korva M, Tul N, et al. Zika virus associated with microcephaly. *N Engl J Med*. 2016;374(10):951-958.

7. Faye O, Freire CCM, Iamarino A, et al. Molecular evolution of Zika virus during its emergence in the 20th century. *PLoS Negl Trop Dis*. 2014;8(1):e2636.

8. Campos GS, Bandeira AC, Sardi SI. Zika virus outbreak, Bahia, Brazil. *Emerg Infect Dis*. 2015;21(10):1885-1886.

9. Lindenbach BD, Rice CM. Molecular biology of flaviviruses. *Adv Virus Res*. 2003;59:23-61.

10. Zanluca C, Melo VC, Mosimann ALP, Santos GI, Santos CN, Luz K. First report of autochthonous transmission of Zika virus in Brazil. *Mem Inst Oswaldo Cruz*. 2015;110(4):569-572.

11. Mécharles S, Herrmann C, Poullain P, et al. Acute myelitis due to Zika virus infection. *Lancet*. 2016;387(10026):1481.

12. Carteaux G, Maquart M, Bedet A, et al. Zika virus associated with meningoencephalitis. *N Engl J Med*. 2016;374(16):1595-1596.

13. Cao-Lormeau V, Blake A, Mons S, et al. Guillain-Barré syndrome outbreak caused by Zika virus infection in French Polynesia [published online February 29, 2016]. *Lancet*. doi:10.1016/S0140-6736(16)00562-6.

14. Woods CG, Parker A. Investigating microcephaly. *Arch Dis Child*. 2013;98(9):707-713.

15. Adibi JJ, Marques ET Jr, Cartus A, Beigi RH. Teratogenic effects of the Zika virus and the role of the placenta. *Lancet*. 2016;387(10027):1587-1590.

16. von der Hagen M, Pivarcsi M, Liebe J, et al. Diagnostic approach to microcephaly in childhood: a two-center study and review of the literature. *Dev Med Child Neurol*. 2014;56(8):732-741.

17. Gérardin P, Sampériz S, Ramful D, et al. Neurocognitive outcome of children exposed to perinatal mother-to-child Chikungunya virus infection: the CHIMERE cohort study on Reunion Island. *PLoS Negl Trop Dis*. 2014;8(7):e2996.

18. Lanciotti RS, Kosoy OL, Laven JJ, et al. Genetic and serologic properties of Zika virus associated with an epidemic, Yap State, Micronesia, 2007. *Emerg Infect Dis*. 2008;14(8):1232-1239.

19. Stadlbauer A, Salomonowitz E, Brenneis C, et al. Magnetic resonance velocity mapping of 3D cerebrospinal fluid flow dynamics in hydrocephalus: preliminary results. *Eur Radiol*. 2012;22(1):232-242.

20. Zucca C, Binda S, Borgatti R, et al. Retrospective diagnosis of congenital cytomegalovirus infection and cortical maldevelopment. *Neurology*. 2003;61(5):710-712.

21. Jaglin XH, Chelly J. Tubulin-related cortical dysgeneses: microtubule dysfunction underlying neuronal migration defects. *Trends Genet*. 2009;25(12):555-566.

22. Romaniello R, Arrigoni F, Bassi MT, Borgatti R. Mutations in α- and β-tubulin encoding genes: implications in brain malformations. *Brain Dev*. 2015;37(3):273-280.

23. Tang H, Hammack C, Ogden SC, et al. Zika virus infects human cortical neural progenitors and attenuates their growth. *Cell Stem Cell*. 2016;18(5):587-590.

24. Corey L, Wald A. Maternal and neonatal herpes simplex virus infections. *N Engl J Med*. 2009;361(14):1376-1385.

25. Müller-Oehring EM, Schulte T, Rosenbloom MJ, Pfefferbaum A, Sullivan EV. Callosal degradation in HIV-1 infection predicts hierarchical perception: a DTI study. *Neuropsychologia*. 2010;48(4):1133-1143.

26. Bosnjak VM, Daković I, Duranović V, Lujić L, Krakar G, Marn B. Malformations of cortical development in children with congenital cytomegalovirus infection: a study of nine children with proven congenital cytomegalovirus infection. *Coll Antropol*. 2011;35(suppl 1):229-234.

27. Hall JG. Arthrogryposis multiplex congenita: etiology, genetics, classification, diagnostic approach, and general aspects. *J Pediatr Orthop B*. 1997;6(3):159-166.

28. Kouamé N, N'goan-Domoua AM, Nikiéma Z, et al. Polyhydramnios: a warning sign in the prenatal ultrasound diagnosis of foetal malformation? *Diagn Interv Imaging*. 2013;94(4):433-437.

29. Baronti C, Piorkowski G, Charrel RN, Boubis L, Leparc-Goffart I, de Lamballerie X. Complete coding sequence of Zika virus from a French polynesia outbreak in 2013. *Genome Announc*. 2014;2(3):e00500-e00514.

30. Besnard M, Lastère S, Teissier A, Cao-Lormeau V, Musso D. Evidence of perinatal transmission of Zika virus, French Polynesia, December 2013 and February 2014. *Euro Surveill*. 2014;19(13).

31. Musso D. Zika virus transmission from French Polynesia to Brazil. *Emerg Infect Dis*. 2015;21(10):1887-1889.

32. McCarthy M. Severe eye damage in infants with microcephaly is presumed to be due to Zika virus. *BMJ*. 2016;352:i855.

33. Ventura CV, Maia M, Bravo-Filho V, Góis AL, Belfort R Jr. Zika virus in Brazil and macular atrophy in a child with microcephaly. *Lancet*. 2016;387(10015):228.